Separation and Purification Technology 301 (2022) 121923

Contents lists available at ScienceDirect

Separation and Purification Technology

journal homepage: www.elsevier.com/locate/seppur

Non-dispersive CO_2 separation process using vacuum desorption and ionic liquids as carbon capture and utilization innovative technology

Jose Manuel Vadillo [*], Lucia Gomez-Coma, Aurora Garea, Angel Irabien

Departamento de Ingenierías Quimica y Biomolecular, Universidad de Cantabria, 39005 Santander, Spain

A R T I C L E I N F O

Keywords:
Carbon capture
Membrane vacuum regeneration
Hollow fiber membrane contactor
Ionic liquids
Process simulation

A B S T R A C T

Slowing down climate change requires urgent measures, and consequently, one of the main challenges of the scientific community is to develop innovative technologies to reduce carbon dioxide emissions to the atmosphere. Non-dispersive CO_2 absorption using ionic liquids (ILs) as solvent and membrane vacuum regeneration (MVR) as desorption step are considered as a one of the most promising technologies for solvent regeneration in post-combustion CO_2 capture and utilization (CCU) since high purity carbon dioxide streams are needed for technical valorization approach. In this work, the chemical binding 1-ethyl-3-methylimidazolium acetate ([emim][Ac]) and the physical solvent 1-ethyl-3-methylimidazolium methyl sulfate ([emim][MS]) have been selected. COSMO based/Aspen Plus methodology has been successfully executed to specify the COSMOSAC property method used in the commercial process simulator (Aspen Plus). Besides, a detailed two-dimensional mathematical model of MVR technology has been validated for the first time with [emim][MS] as a representative of physical ionic liquid solvent. The effect on CO_2 desorbed flux and process efficiency have been tested at different operation conditions in order to compare the behavior of chemical and physical absorption based on ionic liquids. Low vacuum pressure and high temperature show a positive influence in the solvent regeneration process, while high liquid flow-rate increases the process performance but also decrease the CO_2 desorption. The IL ([emim][Ac]) presented higher MVR performance (92 %) than the IL [emim][MS] (83 %) at the best operational conditions (313 K and 0.04 bar), in which the total energy consumption has been estimated on 0.62 and 0.34 $MJ_e \cdot kgCO_2^{-1}$, respectively. These results noted the benefit of the MVR technology based on ILs compared to the conventional amino-based high -temperature regeneration process (1.55 $MJ_e \cdot kgCO_2^{-1}$), presenting a step forward in the substitution of amines. This work provides a valuable tool to help in the decision-making to select the most promising ionic liquids, reducing laboratory efforts and, consequently, experimental costs.

1. Introduction

Efforts to reduce carbon dioxide (CO_2) emissions in industry and energy sectors (decarbonization) are crucial to reach the net-zero greenhouse gas emissions goal by 2050. [1]. In this context, post-combustion Carbon Capture, Utilization, and Sequestration (CCUS) technologies are currently calling attention due to their potential of significantly capturing CO_2 from point sources (e.g., fossil fuel power plants) by different approaches, which involve the carbon capture from the industrial processes output gas to be used for carbon-based products as a resource (CCU) or to permanent storage underground in geological cavities (CCS) [2].

Solvent-based absorption–desorption technology which typically separates CO_2 from flue gas in packing columns is presented as one of the most mature technologies. Nevertheless, the main challenge is to achieve a reduction in the energy consumption for CO_2 rich-solvent regeneration carried out in the desorption column, which is estimated to constitute 15–30 % of the power plant output [3]. Focusing on it, Membrane Vacuum Regeneration technology (MVR) is proposed as an innovative CO_2 desorption process allowing energy savings with respect to conventional packed columns for the CO_2 desorption step [4–7]. Using MVR system, carbon dioxide is desorbed in a hollow fiber membrane contactor (HFMC) from the rich solution by vacuum technology. The application of vacuum for CO_2 desorption reduces the required solvent regeneration temperature and, therefore, the energy consumption to the overall CO_2 capture system [8]. Moreover, the reduced temperatures of the MVR technology increase the applicability of polymeric hollow fiber membrane contactors (HFMC), which have advantages such as low-cost production, hydrophobicity, commercial

---

* Corresponding author.
E-mail address: vadillojm@unican.es (J.M. Vadillo).

https://doi.org/10.1016/j.seppur.2022.121923
Received 9 May 2022; Received in revised form 7 August 2022; Accepted 9 August 2022
Available online 12 August 2022

Nomenclature

P_{CO_2}	CO_2 partial pressure (MPa)
x_{CO_2}	CO_2 molar fraction (–)
T	Temperature (K)
γ_{CO_2}	CO_2 activity coefficient (–)
$A_i.B_i$	Adjusted equation parameters (–)
z	Molar ratio of CO_2 absorbed per mol of ionic liquid (–)
ρ	Density ($kg{\cdot}m^{-3}$)
μ	Viscosity (mPa·s)
MW	Molecular weight ($g{\cdot}mol^{-1}$)
K_H	Henry's Law constant (MPa)
K_H'	Aspen Henry's Law constant (MPa)
K_{eq}	Equilibrium constant (–)
ΔH_R	Enthalpy of reaction ($kJ{\cdot}mol^{-1}$)
W	Electric energy consumption ($MJ_e{\cdot}\ s^{-1}$)
Q_{regen}	Heat energy consumption ($MJ_{th}{\cdot}\ s^{-1}$)
ξ	Energy transfer coefficient (–)
E_T	Energy required to remove 1 kg of CO_2 ($MJ{\cdot}kgCO_2^{-1}$)
q_{CO_2}	Desorbed CO_2 mass-flow ($kgCO_2{\cdot}s^{-1}$)
G_V	Desorbed CO_2 mole-flow ($mol{\cdot}s^{-1}$)
F_V	Desorbed CO_2 flow-rate ($L{\cdot}s^{-1}$)

availability and a wide range of chemical and morphological tunability, being not suitable for higher temperatures of operation [9].

Up to date, the most widely used solvents in CO_2 desorption process based on MVR technology are amine-based solutions, mainly due to the low viscosity, affordable cost and high CO_2 absorption capacity, even if the CO_2 partial pressures are low [7]. In this context, Kosaraju et al. [10] demonstrated the feasibility of CO_2 membrane stripping using commercial PP membrane contactors by long term running (55 days test). Fang et al. [11], Yan et al. [12], and Wang et al. [13] screened 23 types of alkalonamines for MVR and evaluated experimentally the relationship between solvent composition and MVR efficiency. Listiyana et al. [5] performed CO2 regeneration experiments using PP HFMC and activated amines to increase CO_2 regeneration efficiency and to decrease the solvent cost. Pointing out the focus on the energy saving, Nii et al. [14] showed that the MVR technology could effectively employ low-temperature energy or waste heat in the power plants. However, disadvantages have been reported for amine-based CO_2 desorption process, such as absorbent losses and degradability, energy intensive regeneration requirement, and HFMC corrosiveness, which promote the research of alternative solvents with better properties to address these deficiencies [15]. Thus, it is necessary to search for new solvents to overcome the present limitations shown by amines.

In this sense, ionic liquids (ILs) are presented as potential alternatives due to their special features for CO_2 capture like high uptake capacity, negligible vapor pressure, wide operation temperature range and tunable solvent [16,17]. ILs are divided in two main categories, non-functionalized room temperature (RTILs) and task specific (TSILs). The principal difference between these two types resides in that while RTILs behave like typical physical absorbents for gases represented by Henry's Law constant, the TSILs present both physical and chemical absorption and, consequently, may absorb more CO_2. However, the solvent regeneration process using TSILs is very energy-intensive due to chemical bonding [18].

The recent trends focused on CO_2 desorption process by coupled MVR technology using ILs may be resumed in the efforts of: (i) studying IL-based membrane contactors focused on solvent-membrane compatibility (Mulukutla et al. [19] and Bazhenov et al. [20]), and (ii) covering the design, modeling, and experimental facilities for low-temperature CO_2 desorption using different ILs to address the influence of operating variables (Lu et al. [21], Simons et al. [22] and Vadillo et al. [23]). However, there is a lack of data for the influence of the IL nature (physical or chemical absorption) in the solvent regeneration performance, not only based on thermodynamic and kinetic IL properties (e.g., viscosity, CO_2 solubility) but also based in CO_2 desorption process simulations.

Model and simulation data about CO_2 desorption process by MVR technology and ILs with both physical and chemical nature could be helpful to identify the IL key properties, with the purpose of establishing reliable IL selection criteria, considering the IL tunability property, which provides an extra degree of freedom in ILs design [24]. In this context, a custom 2D model for the CO_2 regeneration process by MVR technology using the chemical IL 1-ethyl-3-methylimidazolium acetate [emim][Ac] has been developed in a previous research work and integrated in the commercial simulation software Aspen Plus v11 by COSMO based/Aspen Plus model and application [23]. However, up to date, modeling information about CO_2 desorption by MVR technology using ILs with physical CO_2 absorption has not been widely studied in literature. From the basis of this simulation support, the experimental results of the continuous absorption–desorption process using the physical IL 1-Ethyl-3-methylimidazolium methyl sulfate [emim][MS] reported in our previous publications, have been used to validate the CO_2 desorption model proposed in this work.

This work aims to contribute to the development of a rigorous selection criteria of the ionic liquids in the CO_2 capture scheme, focusing on the study of the CO_2 desorption process based on MVR technology. Besides, in the present study, COSMO based/Aspen Plus methodology is employed in order to: (i) describe chemical and physical CO_2 absorption parameters and (ii) carrying out simulations of the CO_2 desorption process in the commercial simulation tool Aspen Plus v11. The ILs analyzed [emim][Ac] and [emim][MS] have been chosen to be promising candidates as chemical and physical ILs, respectively. The effect of liquid flowrate, temperature, vacuum level and HFMC size are analyzed on the desorption performance and CO_2 desorbed mole-flow. The energy consumption for solvent regeneration is evaluated based on electrical work required to desorb 1 kg of carbon dioxide from the ILs studied and compared to the energy requirements in the conventional high temperature desorption based on amines. This evaluation intends to help the reader to choose between different types of ILs, which provides a blueprint for solvent selection in the field of the non-dispersive absorption–desorption process using membrane contactors as a promising carbon capture technology.

2. Methodology

This section explains in detail the materials and methods for the experimental procedure of the membrane vacuum regeneration model and simulation approach, the ionic liquids definition task and the desorption energy consumption calculations.

2.1. Experimental: Materials and method

A polypropylene hollow fiber membrane contactor (HFMC) supplied by Liqui-Cel Membrane Contactor (USA) is used to continuous absorption–desorption process. Table 1, shows the specifications of this HFMC. The feed gas of the CO_2 capture system is composed of 15 % carbon dioxide (99.7, Air Liquide, Madrid, Spain) and 85 % nitrogen (99.9 %, Air Liquide, Madrid, Spain), which is in the range of a typical coal-fired power plant (10–16 %) [25].

The IL 1-Ethyl-3-methylimidazolium methyl sulfate [emim][MS] (≥95 %) supplied by Sigma Aldrich has been selected due to its high values of surface tension, contact angle, moderate values of viscosity and the presence of only physical absorption which potentially decrease the energy consumption during the solvent regeneration process [26,27]. The process performance has been compared with previous works using the IL 1-ethyl-3-methylimidazolium acetate [emim][Ac] (≥90 %),

Table 1
Hollow fiber membrane contactor (HFMC) characteristics (Liqui-Cel Membrane Contactor, Minneapolis, Minnesota, USA).

Parameter	**value**
Membrane Material	Polypropylene
Module configuration	Parallel
Module i.d., d_{cont} (m)	25×10^{-3}
Fiber outside diameter, d_o (m)	3×10^{-4}
Fiber inside diameter, d_i (m)	2.2×10^{-4}
Fiber length, L (m)	0.115
Number of fibers, n	2300
Effective inner membrane area, A (m^2)	0.18
Membrane thickness, δ (m)	4×10^{-5}
Membrane pore diameter, d_p (m)	4×10^{-6}
Porosity, ς (%)	40
Packing factor, φ	0.39
Tortuosity, τ	2.50

which presents both physical and chemical absorption [23]. Table 2 shows the chemical formula and structure of both ILs used in this work, chemical [emim][Ac] and physical [emim][MS].

A continuous absorption–desorption setup suitable for CO_2 capture with ILs has been developed as shown in Fig. 1. Operating conditions are presented in Table 3. The IL is recirculated in a closed loop through the lumen side of both HFMCs (absorber and desorber). A digital gear pump (Cole-Parmer Gear Pump System, Benchtop Digital Drive, 0.017 ml/rev, 220 VAC, Spain) has been used to maintain a constant IL flowrate and avoid fluctuations. Experiments have been also performed inside an oven for a controlled temperature environment and isothermal conditions during the absorption–desorption process operation. The feed gas mixture is introduced in counter-current at nearly atmospheric pressure through the shell side of the absorber HFMC in open loop conditions with constant flowrate while the IL passes through the lumen side of the HFMC absorbing the CO_2. The CO_2-rich IL during recirculation is pumped into the tube side of the HFMC desorber where the CO_2 could be regenerated from the rich solution due to the positive effects of reduced pressure applied on the shell side by using a vacuum pump PC 3001 VARIO PRO (Vacuubrand). CO_2 permeated from the rich solution to the shell side through the gas-filled membrane pores and the CO_2 desorbed is measured at the vacuum pump output. Gas mass flowmeters (Alicat scientific, Spain) and a CO_2 analyzer (Geotech, G110 0–100 %, UK) are used to measure the mass flowrate and the CO_2 concentration of the gas streams (feed gas, clean gas and CO_2 output), respectively.

The ILs are recirculated until reaching steady-state (constant CO_2 concentration at the gas side outlet). All the experiments have been carried out three times to obtain reproduced results. These results provided the average values for the set of three experiments, being the experimental error within ± 5 %.

2.2. *Modelling approach*

A rigorous model has been developed in detail in a previous work based on a two-dimensional approach to characterizes the MVR system explained in the previous Section 2.1. *Experimental: Materials and method.* Characteristics of the HFMC considered in the system and operation conditions are described in Table 1 **and** Table 3, respectively. The model developed for CO_2 desorption using MVR technology and ILs, has been validated in a previous work with the chemical absorbent IL [emim][Ac]. In this work, the model developed is rearranged and validated with experimental results using the IL [emim][MS], which is a physical absorbent of CO_2. The following assumptions have been made based on the previous works [7] to find a balance between the experimental prediction results and the model complexity: (i) steady-state and isothermal conditions; (ii) a fully developed parabolic laminar velocity profile is applied on the tube side; (iii) negligible axial dispersion on the tube side; (iv) the [emim][MS] concentration is kept constant throughout the process and (v) negligible pressure drop on the shell side. The schematic diagram of the CO_2 transport in the desorption of CO_2 in the membrane contactor using [emim][MS] is shown in Fig. 2.

The desorption model takes into account that the concentration of CO_2 in the liquid through the module is conditioned to the mass transfer in the gas–liquid interface. The steady-state continuity equations for the CO_2 with simultaneous diffusion within each fiber:

$$V_z \frac{\partial C_{CO_2}}{\partial Z} = D_{CO_2,l}\left(\frac{\partial^2 C_{CO_2}}{\partial r^2} + \frac{1}{r}\frac{\partial C_{CO_2}}{\partial r}\right) \tag{1}$$

where V_z ($m \cdot s^{-1}$) is the liquid velocity in the axial direction; C_{CO_2} ($mol \cdot m^{-3}$) is the physically dissolved CO_2 concentration in the liquid side; and $D_{CO_2,l}$($m^2 \cdot s^{-1}$) is the CO_2 diffusion coefficient in the liquid. The boundary conditions used to solve the model are expressed as follows:

$$C_{CO_2} = C_{CO_2,0} \quad \text{for } Z = 0 \tag{2}$$

$$\frac{\partial C_{CO_2}}{\partial r} = 0 \quad \text{for } r = 0 \tag{3}$$

$$D_{CO_2,l}\frac{\partial C_{CO_2}}{\partial r} = k_{ex}\left(C_{CO_2,g} - \frac{C^*_{CO_2,l}}{\frac{m}{E}}\right) \quad \text{for } r = Ri \tag{4}$$

where $C_{CO_2,0}$ is the physically dissolved CO_2 concentration in the liquid phase at initial time; $C_{CO_2,g}$ is the gas phase CO_2 concentration ($mol \cdot m^{-3}$); $C^*_{CO_2,l}$ is liquid phase CO_2 concentration in the gas–liquid interface; k_{ex} ($m \cdot s^{-1}$) is the combination of the mass transfer coefficients of CO_2 in the membrane and in the gas phase; and the distribution factor (m) is the relation between the CO_2 concentration in the ionic liquid and the CO_2 concentration in the gas phase. This value can be expressed by equation (5) [28] where ρ_l is the molar density of the IL ($mol \cdot L^{-1}$); and H_{CO_2} (MPa) is the Henry constant of CO_2 in [emim][MS].

$$m = \frac{\rho_l RT}{H_{CO_2}} \tag{5}$$

In this work, the enhancement factor (E), which quantifies how the mass transfer is enhanced by the presence of a physico-chemical interaction between the CO_2 and the IL, has been obtained from the literature [29].

2.3. *Components definition and properties*

COSMO-based/Aspen Plus model is used to the CO_2 desorption process using MVR technology and ILs. The pure IL and the CO_2-IL reaction products are introduced into AP by the COSMOSAC property method (in code 1) [30]. Two approaches have been followed to include

Table 2
Abbreviation, name and chemical structure of the 2 ILs studied.

Abbreviations	**Name**	**Formula**	**Chemical structure**
[emim][Ac]	1-ethyl-3-methylimidazolium acetate	$C_7H_{14}N_2O_4S$	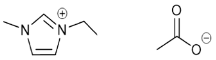
[emim][MS]	1-ethyl-3-methylimidazolium methylsulfate	$C_8H_{14}N_2O_2$	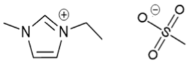

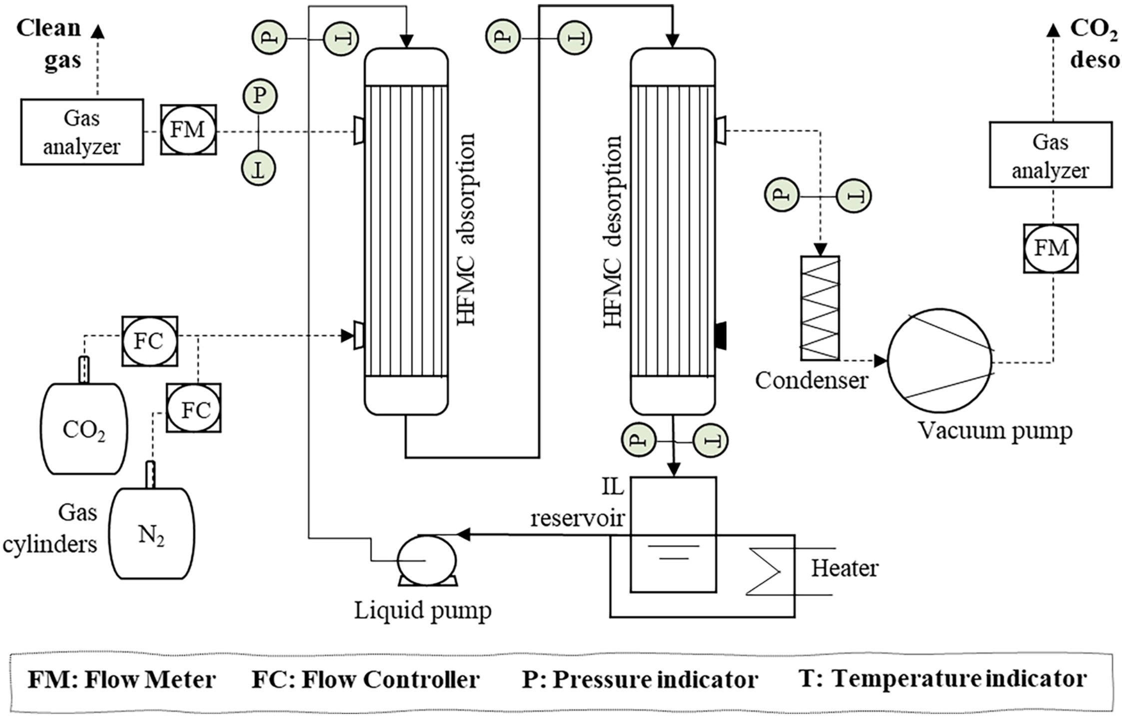

Fig. 1. Experimental setup of the CO_2 absorption–desorption process with one absorption HFMC and one desorption HFMC for MVR. Gas flow (dashed lines), Liquid flow (solid lines).

Table 3
Operating conditions of the absorption–desorption process based on the non-dispersive gas–liquid HFMC contactors, laboratory scale.

Parameter/Property	Value	Unit
Volume, V	100	mL
Temperature, T	289–310	K
Feed Gas flow rate, F_g	60	$mL{\cdot}min^{-1}$
Liquid flow rate, F_l	60	$mL{\cdot}min^{-1}$
Feed gas pressure, $P_{g,in}$	1.03	bar
Liquid pressure, $P_{l,in}$	1.31	bar
Vacuum pressure, P_v	0.04–0.5	bar

the ILs studied in this work into the Aspen Plus v11 process simulator: (i) the [emim][MS] is incorporated employed the ILUAM (C + A-EQ) database since has been recently published with information available for 100 common physical ILs [31]; and (ii) the [emim][Ac] and their reaction products are introduced as pseudo-components into the simulator along with all parameters needed to describe their CO_2 physical and chemical interactions by following the multi-scale COSMO-based/Aspen Plus methodology supported with experimental data and described in detail in a previous work [32]. As summary, to define the COSMOSAC property method for Aspen Plus simulations, quantum chemical structure optimizations and COSMO-RS calculations of the [emim][Ac] and their reaction products are executed. Moreover, to describe the CO_2 mass transfer kinetics, the experimental temperature dependent ILs viscosity data, which is temperature dependent, is added into the Aspen Properties [33]. Finally, to perform the chemical absorption of CO_2 in the selected IL [emim][Ac] using Aspen Plus, CO_2-IL experimental absorption isotherms are successfully fitted to a thermodynamic model in which the physical absorption is described by Henry's Law and the chemical equilibrium reaction considers the stoichiometry of reaction depending on the IL (1:1 mechanism for AHA-ILs and 2:1 mechanism for [emim][Ac]) as explained elsewhere [34].

The gaseous components (CO_2 and N_2) have been included in the simulation as conventional compounds, and their parameters and properties are loaded from Aspen Plus database and completed by the thermophysical properties by following also the multi-scale COSMO-based/Aspen Plus methodology. Table 4 includes the ILs physical and chemical properties estimated by this COSMO-based/Aspen Plus approach.

2.4. *Process simulation*

Coupled membrane technology and ILs have been studied in the recent years in order to improve the overall CO_2 capture system by reducing the regeneration energy consumption of conventional high temperature stripping, which consists of a large size column stripper or a flash unit in adiabatic conditions where the CO_2 is desorbed from the IL at low pressure (0.1 bar) and high temperatures (100 °C) [36]. Although IL with physical absorption of CO_2 has been proposed as a promising alternative to chemical IL absorbents due to the potential to reduce the energy consumption and increase the regeneration performance, most simulation works on the CO_2 capture with physical IL have been focused on the CO_2 absorption stage while very limited research are covered the CO_2 desorption process. This work is focused on the pseudo steady-state solvent regeneration simulation using a HFMC module as shown in Fig. 3, which is part of the non-dispersive absorption–desorption process main flowsheet (Fig. 1). The CO_2 desorption is designed as a MVR technology and the performance is evaluated in Aspen Plus v11 using the user model imported for the CO_2 desorption with MVR technology and IL [emim][Ac] proposed by our previous work [7], following the Aspen Tech guideline and the multi-scale COSMO-based/Aspen Plus methodology, which brings the possibility to import a user model from Aspen Custom Modeler (ACM) to the simulation software Aspen Plus [33]. The use of this custom model for the physical IL [emim][MS] provided the capacity to compare both physical and chemical IL in terms of desorption performance and CO_2 desorbed flux at different operational conditions. For this purpose, several experiments at different operational conditions have been carried out as (described in Section 2.1. *Experimental: Materials and method*) for model validation using [emim][MS] as absorbent in a steady-state solvent regeneration unit based on MVR technology.

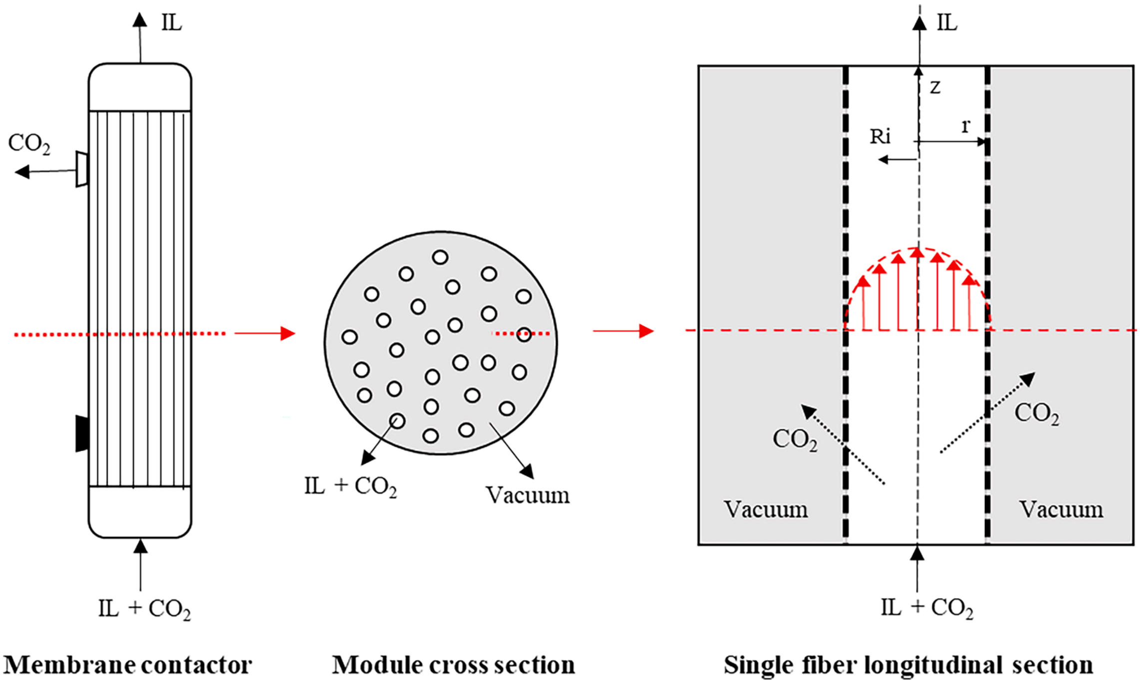

Fig. 2. Diagram of CO_2 MVR process in a hollow fiber membrane contactor (HFMC).

Table 4
Physical and chemical properties of selected IL estimated by COSMO-based/ Aspen Plus approach at 313 K and 1 bar: molar weight (MW), density (ρ), viscosity (μ), Henry (K_H) and reaction equilibrium (Keq) constant.

Ionic liquid	MW ($g \cdot mol^{-1}$)	ρ ($kg \cdot m^{-3}$)	μ (mPa·s)	K_H (Mpa)	Keq	Reference
[emim][Ac]	170.2	1137.6	42.6	10.6	89.67	[33]
[emim][MS]	222.3	1265.8	44.9	6.5	–	[35]

Both physical IL [emim][MS] and chemical IL [emim][Ac] evaluated in this work as absorbents are compared using the polypropylene HFMC (Table 1) in terms on solvent regeneration performance and CO_2 desorbed flow. The parameters and operating conditions for the simulations have been taken from the experimental set up conditions described in Table 3. The liquid (H-RICHIL) stream composition is fully described by two compounds (CO_2 absorbed into IL). This liquid stream, which is the output of the absorption stage, is constantly pumped into the tube side of (DES-01), where the CO_2 is desorbed from (H-RICHIL) to (H-CO2OUT), due to the pressure gradient created in the shell side of (DES-01) by the vacuum applied, while the regenerated IL (H-LEANIL) is pumped again to the absorption stage. The CO_2 desorbed is compressed to 2 bar which has been set for further CO_2 utilization [37]. Three key assumptions have been considered in the simulation of the CO_2 regeneration stage: (i) isothermal and steady-state conditions; (ii) constant IL concentration and (iii) pressure drop on the membrane contactor negligible.

In this study, the CO_2 desorbed flux and CO_2 desorption efficiency are used to test the IL regeneration performance in HFMC based on MVR technology. The CO_2 desorption efficiency can be calculated by the equation:

$$\text{Desorption eff. } (\%) = \frac{\alpha_{\text{rich}} - \alpha_{\text{lean}}}{\alpha_{\text{rich}}} \times 100 \tag{6}$$

where α_{rich} and α_{lean} are the CO_2 loading in the IL $\left(\frac{mol_{CO_2}}{mol_{IL}}\right)$ before and after, respectively, of one pass of IL through the HFMC.

The CO_2 desorbed flux (G_V, $mol \cdot s^{-1} \cdot m^{-2}$) is calculated as:

$$G_V = \frac{F_V}{v_m A} \tag{7}$$

where F_V is the CO_2 flowrate desorbed from the MVR module measured on the vacuum pump output ($L \cdot s^{-1}$), v_m is the molar volume of CO_2 ($L \cdot molCO_2^{-1}$, STP conditions) and A is the specific membrane area (m^2).

2.5. Energy consumption

The energy requirement for solvent regeneration with MVR technology has been estimated at different operational conditions (vacuum pressure and temperature) using both chemical IL [emim][Ac] and physical IL [emim][MS]. The energy consumption calculations carried out in this section are key to solvent selection task, for comparing both chemical and physical absorbents in the CO_2 desorption stage specifically, which is the main energy consuming process operation. Additionally, the energy requirement results play a fundamental role on the techno-economic analysis of the MVR technology to reach a trade-off between performance-energy cost and to compare with conventional regeneration methods. In this case, the assumptions are taken into account based on literature [32]: (i) only the CO_2 desorption stage as described in Fig. 3 is addressed in energy requirements calculations since it will be compared to the conventional desorption process; Gas-powered blower and liquid pump are not considered; (ii) compression process (COMP-01) is isentropic. The CO_2 desorbed (H-CO2OUT) is compressed to 2 bar, which is considered a referenced value of output pressure of CO_2 desorption process [38]. (iii) only reaction heat duty (for chemical IL) and the extra work for the vacuum pump and the compression unit are analyzed. The energy required for solvent evaporation (latent heat, Q_{latent}) has not been included since non-volatile IL is used as absorbent. Moreover, considering the possibility of use waste heat to increase the temperature of the IL up to 313 K (maximum temperature in this work), the energy required for solvent heating (sensible heat, Q_{sens}) has not considered in calculations [33].

Because of the temperature required for MVR process is lower compared to the thermal regeneration, it is more equitable to compare energy consumption with regeneration heat duty by total equivalent work [39]. Furthermore, to remove 1 kg of CO_2, the total energy

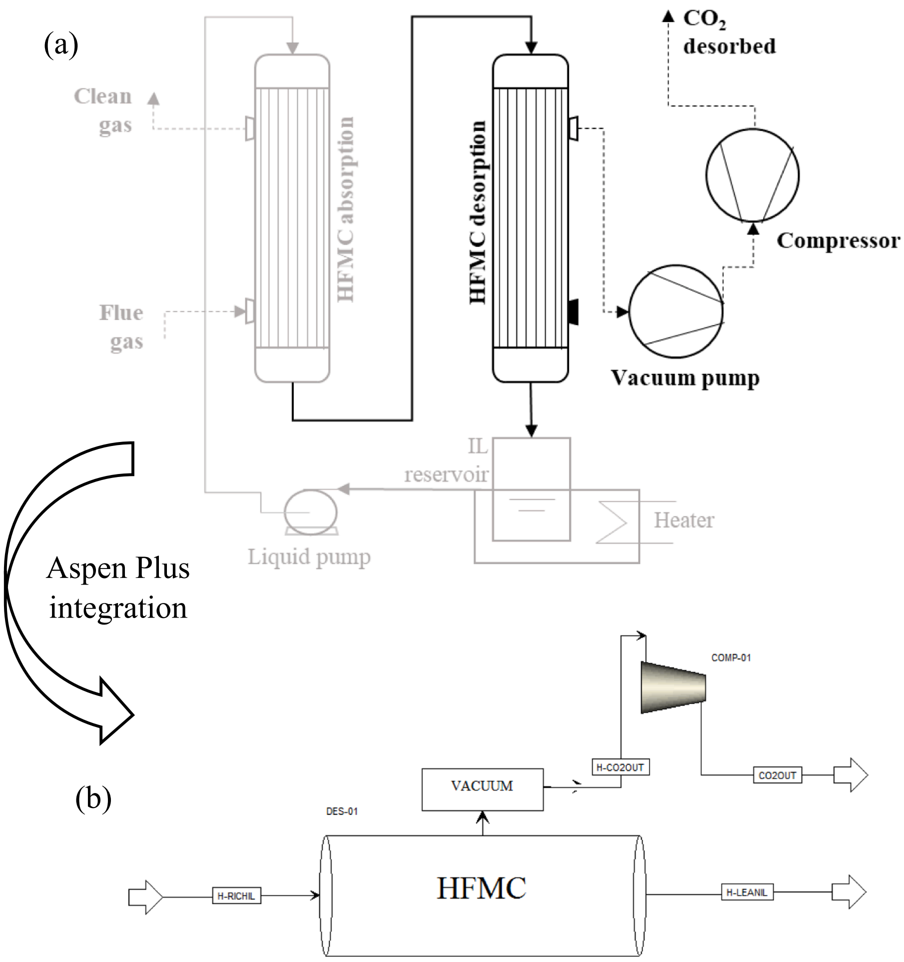

Fig. 3. Membrane vacuum regeneration process flowsheet (a), and its implementation in the in Aspen Plus simulation tool (b).

consumption in terms of work required (E_T, $MJ_e \cdot kgCO_2^{-1}$) is calculated by equation (8) as the sum of the work needed for vacuum pump W_{vp}, vacuum pump cooling W_{cool}, compressor W_{comp} ($MJ_e \cdot s^{-1}$) and the equivalent work of the reaction heat duty W_{regen} ($MJ_e \cdot s^{-1}$) described in equation (9). Here, q_{CO_2} is the desorbed CO_2 mass flowrate ($kgCO_2 \cdot s^{-1}$), Q_{regen} is the reaction heat duty, which is the total heat required for reversing the reaction and releasing the CO_2 from the chemical IL ($MJ_{th} \cdot s^{-1}$) [40], and ξ is the energy transfer efficiency from heat to electric energy, which is assigned according literature available to 0.4 [41,42].

$$E_T = \frac{(W_{vp} + W_{comp} + W_{cool} + W_{regen})}{q_{CO_2}} \tag{8}$$

$$W_{regen} = \xi \hat{A} \cdot Q_{regen}, \tag{9}$$

It may be noted that the total energy consumption is represented by the "e" abbreviation because is based on the electrical energy (W_i), while thermal regeneration energy required is presented by the "th" abbreviation in view of the fact that is based heat energy (Q_i). Furthermore, the energy transfer efficiency (ξ) is used to convert the heat energy Q_{regen} ($MJ_{th} \cdot s^{-1}$) to electric energy W_{regen} ($MJ_e \cdot s^{-1}$) in order to estimate the total energy consumption E_T ($MJ_e \cdot kgCO_2^{-1}$).

The regeneration energy Q_{regen} can be calculated by equation (10) where ΔH_{CO_2} ($MJ_{th} \cdot kmolCO_2^{-1}$) is the enthalpy of the CO_2-IL chemical reaction collected from available literature [34]; and PM_{CO_2} ($kgCO_2 \cdot kmolCO_2^{-1}$) is the CO_2 molecular weight.

$$Q_{regen} = \frac{\Delta H_{CO_2}}{PM_{CO_2}} * q_{CO_2} \tag{10}$$

The work required for the vacuum pump (W_{vp}) is calculated by equation (11) [8], while the performance is described according to equation (12) [11].

$$W_{vp} = \frac{G_V RTZ\kappa}{(\kappa - 1)\eta_{VP}} \left[\left(\frac{P_{VP,out}}{P_{VP,in}} \right)^{\frac{(\kappa-1)}{Z\kappa}} - 1 \right] \tag{11}$$

$$\eta_{vp} = 0.1058 ln \left(\frac{P_{VP,out}}{P_{VP,in}} \right) + 0.8746, \tag{12}$$

Here, $P_{VP,in}$ (bar) is the shell side vacuum pressure (permeate); $P_{VP,out}$ (bar) is the atmospheric pressure; G_V is the molar flowrate of the desorbed CO_2; κ is the adiabatic constant; and Z is compression stage number. The work for cooling the vacuum pump (W_{cool}), which relies on the equations (11) and (12), is described by equation (13):

$$W_{cool} = 0.054 \eta_{VP} W_{VP} \tag{13}$$

The compressor work requirement (W_{comp}) is estimated by a pressure rise simulation (from 1 to 2 bar) in the (H-CO2OUT) using the isentropic compressor model from Aspen Plus software (P-02).

The energy consumption terms for the proposed MVR technology have been analyzed in detail as a substitute to conventional packed columns under an industrial framework in our previous work [33]. It is estimated up to a 30 % reduction of the solvent regeneration by MVR technology compared to the typical thermal desorption process in large scale applications.

In this work, the energy consumption of the CO_2 desorption based on MVR technology is compared in terms of chemical or physical interactions between ILs and CO_2. The results provided in the next section, allows to identify possible advantages of ILs according to their nature in the CO_2 capture system, attending to the CO_2 desorption stage, which is the most energy intensive operation.

3. Results and discussion

This section explains in detail the results related to the MVR model validation based on the experimental results. Moreover, a rigorous parametric evaluation has been developed to study the process performance and the energy requirement in the cases of different operation parameters and ILs.

3.1. Absorption properties and model validation

The imidazolium ILs [emim][Ac] and [emim][MS] have been evaluated in this work for CO_2 regeneration process as chemical and physical CO_2 absorbents, respectively. As described in Table 4 previously, COSMO-based/Aspen Plus methodology has been applied for pure IL and IL-CO2 mixture properties estimation. These estimated thermodynamic and kinetic properties supplied the Aspen Plus simulation framework of the IL capacity for CO_2. The parameters calculation and validation procedures for the chemical IL [emim][Ac] using COSMO-based/Aspen Plus methodology has been detailed in our previous work [33] while property estimation for physical IL [emim][MS] has been reported by Ferro et al. [35].

The equilibrium isotherms of the [emim][Ac]–CO_2 and [emim][MS]–CO_2 interactions have been reported by Shifflet et al. [43] and Yim et al. [44], respectively. According to its isotherms, the IL [emim][Ac] shows better absorption capacity than [emim][MS], particularly at low CO_2 partial pressures, which is where the post-combustion CO_2 capture system operate. The IL [emim][MS] is a suitable absorbent for this system at higher partial pressures based mainly in two statements: (i) its good absorbent parameters (low viscosity and volatility); and (ii) its behavior as a physical CO_2 absorbent, which potentially can be completely regenerated.

The custom model (described in depth in section *2.2. Modelling approach*) has been validated for [emim][MS] by comparison between simulated and experimental results of regeneration performance described by equation (6) at different operation conditions of vacuum pressures and temperatures. The experimental setup is described in Section 2.1. *Experimental: Materials and method*, and the main membrane characteristics and the process conditions have been adopted from Table 1 and Table 3, respectively. In this sense, Table 5 shows the influence of the operating parameters on the desorption efficiency and the values of the standard deviation of the model, calculated by the following equation:

$$deviation(\%) = \frac{|experimental - model|}{experimental} * 100 \tag{14}$$

In addition, in order to provide a graphical representation of the overall standard deviation of the model, Fig. 4 shows the process performance results at different operating conditions estimated and calculated experimentally using the IL [emim][Ac] and IL [emim][MS].

The circle dots represent the desorption efficiencies using the IL [emim][MS] and the triangle dots represent the corresponding to the IL [emim][Ac]. The relative standard deviations between simulation results and experimental data points are in the range of ± 15 %. Taking into account these results, the model assumptions (listed in Section 2.2. *Modelling approach*) have been validated for both ILs based on the agreement between modeled and experimental results. Considering that the model has been validated, it is further used in the simulation tool AP to study the effect of operational parameters and IL nature in the CO_2 desorption performance by using both physical and chemical ILs.

Table 5
Influence of operating parameters (vacuum pressure and temperature) on desorption efficiency and standard deviation of estimated values.

		[emim][Ac]; Desorption efficiency (%)		
Pv (bar)	**T (K)**	**Experimental**	**Simulated**	**Deviation (%)**
0.50	**289**	2.3	2.5	−8.7
0.50	**313**	10.6	11.1	−4.7
0.20	**289**	60.7	60.7	0.0
0.20	**313**	77.8	76.4	1.8
0.04	**289**	91.4	86.6	5.2
0.04	**313**	93.8	87.5	6.7

		[emim] [MS] ; Desorption efficiency (%)		
Pv (bar)	**T (K)**	**Experimental**	**Simulated**	**Deviation (%)**
0.20	**289**	13.8	13.9	−0.8
0.20	**313**	16.1	16.1	−0.1
0.10	**289**	47.0	45.7	2.7
0.10	**313**	54.8	52.9	3.4
0.04	**289**	76.8	65.6	14.5
0.04	**313**	86.9	75.0	13.7

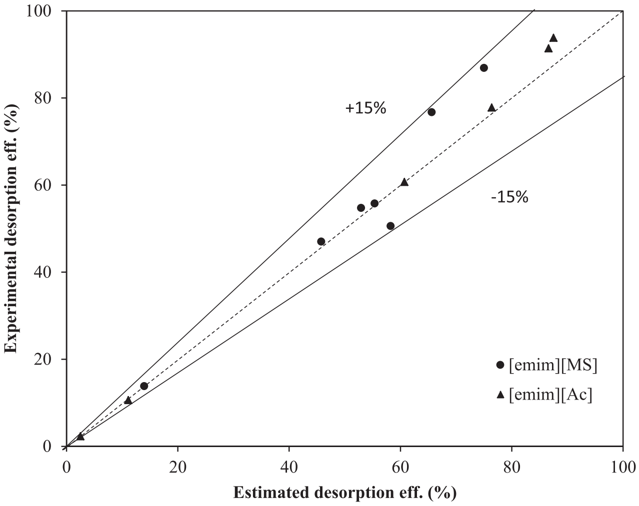

Fig. 4. CO_2 desorption model validation by comparison of the experimental and estimated desorption performance using both chemical IL [emim][Ac] and physical IL [emim][MS].

3.2. Parametric study

The capacity of the COSMO-RS calculations to estimate both chemical ILs [25,32] and physical ILs [45] properties for certain anion/cations sets and the CO_2 regeneration 2D-model validation using the studied IL ([emim][Ac] and [emim][MS]) have been investigated. According to literature, the chemical IL [emim][Ac] seems to be better solvent than physical IL [emim][MS] for post-combustion CO_2 capture system if only CO_2 solubility results have been analyzed since chemical reaction promotes the absorption of CO_2 into the IL at low partial pressures [44]. However, the process performance not only depends on the chemical and/or physical interactions between IL and CO_2, but also the mass transfer coefficients, the operation conditions (vacuum pressure, temperature, solvent flow rate and module length) and the main characteristics of the membrane contactor such as fluid dynamics and membrane geometry [46].

The next part of this work debates the simulation results (CO_2 desorption efficiency and CO_2 desorbed flux) with both chemical and physical ILs at different operation conditions of the IL desorption stage using the COSMO-based/Aspen Plus methodology as shown in Fig. 3. This simulation approach may be applied to further studies of solvent selection in terms of cost and process performance.

The base case scenario in terms of process parameters has been selected according to the highest efficiency calculated for the CO_2 regeneration process (reported on Table 5) by using one HFMC (module parameters described in Table 1) and both ILs chosen. In this sense, the temperature of solvent and the process vacuum pressure has been defined as 313 K and 0.04 bar, respectively.

The results when varying the operation vacuum pressure have been analyzed in Fig. 5. Lower CO_2 partial pressure (higher vacuum applied) on the permeate side of the HFMC, promotes the CO_2 mass transfer driving force through the membrane, which increases the desorption performance as a result of the higher CO_2 desorbed rate. However, to avoid wetting phenomena, it is recommended to keep the permeate side vacuum pressure higher than 0.035 bar. Furthermore, only chemical [emim][Ac] is able to reach a target of 90 % desorption performance for this MVR system using one membrane contactor (HFMC characteristics described in Table 1). Two main points could be remarked from the results shown in Fig. 5: (i) Chemical IL [emim][Ac] is less sensitive to vacuum pressure conditions (lower slope), which could be explained by the fact that chemical IL requires more energy to break the CO_2-IL chemical bond; (ii) Physical [emim][MS] needed CO_2 partial pressures lower than 0.2 bar to desorb CO_2 at this operating temperature. This could be explained due to the lower CO_2 loading capacity of physical ILs that decreased the CO_2 driving force through the membrane resulted in higher vacuum level required. Moreover, Physical IL [emim][MS] required the application of high vacuum to reach the same desorption efficiency than that with chemical IL [emim][Ac], which increased the energy consumption for both units operation, the vacuum pump and compressor, and thus the overall cost of the desorption system based on MVR technology [33]. The energy consumption evaluation at different values of liquid temperature and CO_2 desorption vacuum pressure will be discussed in Section 3.3. *CO_2 desorption: Energy consumption.*

The influence of liquid absorbent temperature on CO2 regeneration performance is described in Fig. 6. The MVR efficiency increases with greater solvent temperature until a constant desorption performance is reached. This behavior in both ILs studied could be explained by the lower viscosity (μ) at higher temperatures, which enhance the diffusion of CO_2 into the IL since the mass transfer coefficient is mainly governed by liquid phase mass transfer resistance. Physical IL [emim][MS] shows lower CO_2 desorption performance and CO_2 desorbed flux at the range of temperatures simulated (273–373 K), which is mainly explained due to lower CO_2 capacity of the physical IL that leads to lower CO_2 driving force through the membrane. Since the maximum desorption performance simulated is 97 % for chemical IL [emim][Ac] and 83 % for

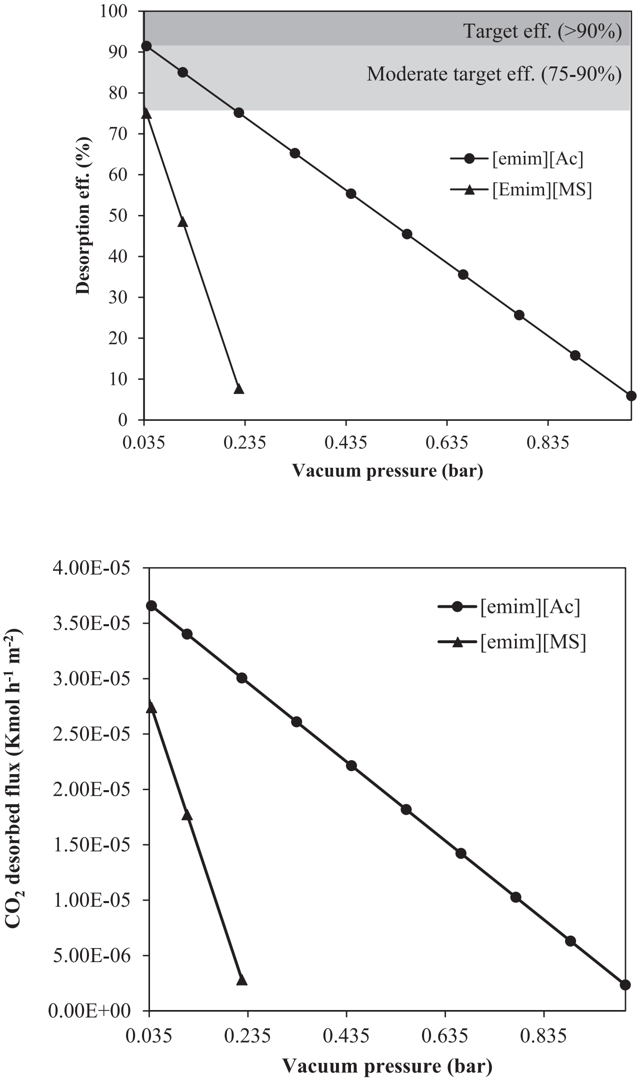

Fig. 5. Desorption efficiency (a) and CO_2 desorbed flux (b) by using 2 ILs at different vacuum pressure. Commercial HFMC process parameters: temperature 313 K, liquid flowrate 60 ml·min^{-1}.

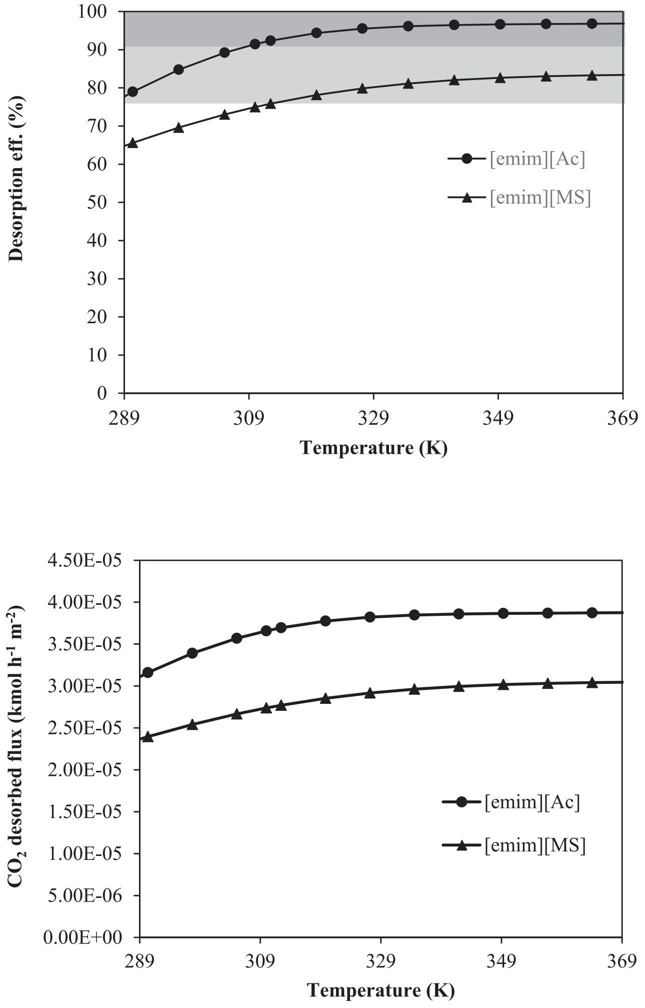

Fig. 6. Desorption efficiency (a) and CO_2 desorbed flux (b) by using 2 ILs at different temperatures. Commercial HFMC process parameters: vacuum pressure 0.04 bar, liquid flowrate 60 ml·min^{-1}.

physical IL [emim][MS], the desorption process efficiency target of 90 % is achieved only by [emim][Ac] at 307 K, while a more moderate desorption (75 % as reference) is obtained by [emim][MS]. Although simulation results have been evaluated in a wide range of temperatures, temperatures higher than 313 K may require more resistant HFMC membrane materials due to thermal and chemical constraints of the commercial polypropylene HFMC used in our work.

The influence on the desorption performance of CO_2-rich IL mole-flow is shown in Fig. 7. Lower liquid mole-flow increased the CO_2 desorption efficiency, due to the increase of the residence time across the membrane contactor fibers, which increase the capability of the CO_2 to be desorbed from the CO_2-rich IL. The same trend in CO_2 desorption efficiency at different IL mole-flow is described in both chemical and physical ILs. However, the mole-flow decrease of the CO_2-rich IL leads to a lower CO_2 desorbed mole-flow (around one order of magnitude) and higher equipment size required, which increase the total capital cost of the overall capture system. Taking into account these effects, the optimal liquid flow rates should be estimated by searching a trade-off between the desorption process performance, the CO_2 desorbed mole-flow and the overall process cost.

Finally, considering a multi-HFMC approach, the CO_2 desorption performance has been analyzed in Fig. 8 by the increase of the contact area (increasing the number of HFMC operated in series) at the same process conditions with both ILs. The estimated number of contactors required to reach the maximum desorption performances with both ILs (97 % for chemical IL [emim][Ac] and 83 % for physical IL [emim][MS]), are two and three HFMC, respectively. However, if the process efficiency target is 90 %, the chemical IL [emim][Ac] needed only 1 module while physical IL [emim][MS] could not reach that value at the operational conditions studied in this work.

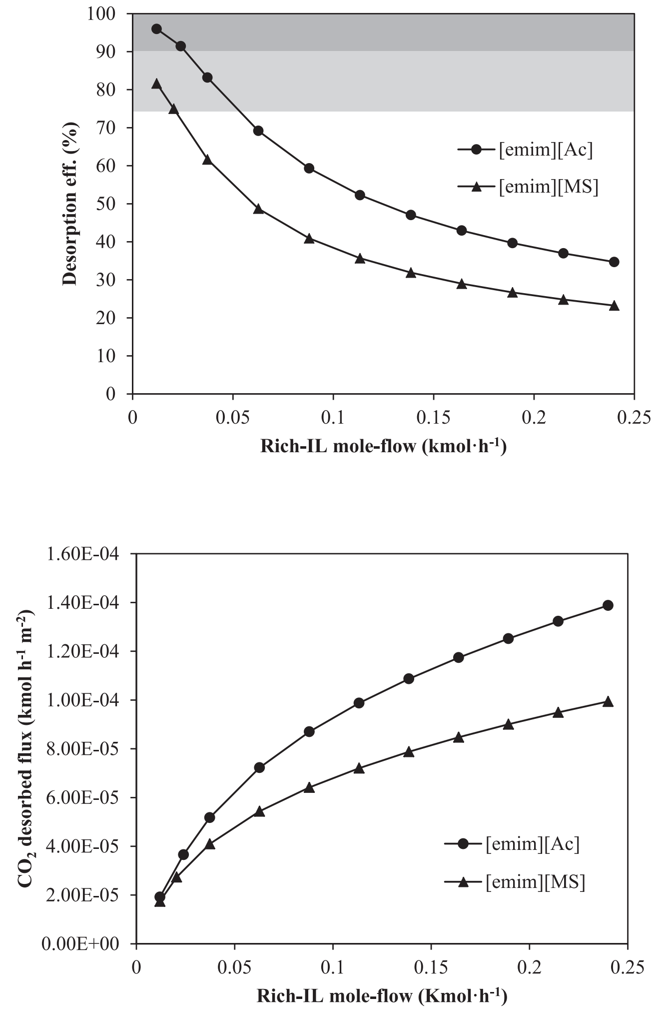

Fig. 7. Desorption efficiency (a) and CO_2 desorbed flux (b) by using 2 ILs at different CO_2-rich IL mole-flow. Commercial HFMC process parameters: temperature 313 K, vacuum pressure 0.04 bar.

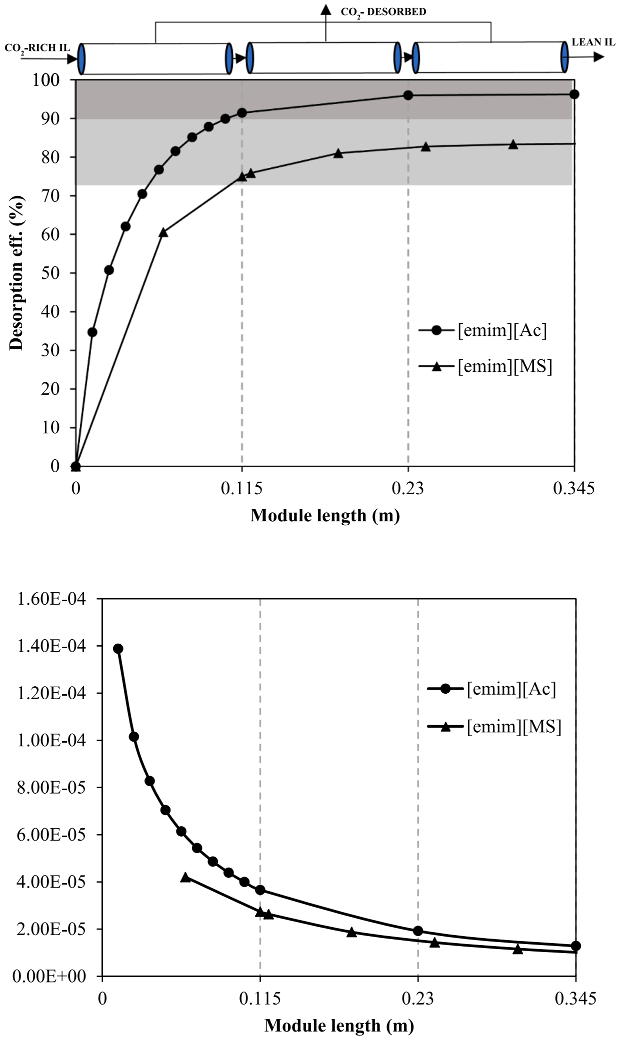

Fig. 8. Desorption efficiency (a) and CO_2 desorbed flux (b) by using 2 ILs at different CO_2-rich IL mole-flow. Commercial HFMC process parameters: temperature 313 K, vacuum pressure 0.04 bar.

Summarizing, the chemical IL [emim][Ac] shows better CO_2 regeneration performance and higher CO_2 desorbed flux than the physical IL [emim][MS] at different vacuum pressures, liquid temperature, liquid flowrate and module length. This could be explained mainly due to the larger capability of CO_2 to be absorbed into chemical IL by chemisorption, which increases the CO_2 driving force through the membrane in the CO_2 regeneration system based on MVR technology.

However, the total energy consumption of MVR system (ET, $MJ_e\cdot kgCO2^{-1}$) with chemical ILs such as [emim][Ac] may be expected to be higher than physical ILs such as [emim][MS] due to the extra energy required to reverse the CO_2-IL chemical reaction as previously reported [29,47]. At this point, the energy consumption analysis is important to contribute to the better IL selection for the CO_2 Capture system. For this purpose, the CO2 regeneration energy consumption using MVR technology with both chemical and physical ILs is evaluated in the following section.

3.3. CO_2 desorption: Energy consumption

As considered in Section 2.5 *Energy consumption*, the total energy required for the desorption stage based on MVR technology (E_T, $MJ_e \cdot kgCO_2^{-1}$) has been calculated from the aggregate of the work required for the correct operation of the three process units (the vacuum pump, W_{vp}; the vacuum pump cooling, W_{cool}; and the compressor, W_{comp}), and the equivalent regeneration work (W_{regen}), for the case in which the CO_2-IL chemical reaction occurs. Fig. 9 shows the required work contribution using two ILs with different nature in terms of CO_2 absorption, the chemical IL [emim][Ac] and the physical IL [emim][MS]). For the calculations, four representative operating conditions of vacuum pressure (0.04 and 0.22 bar) and temperature (289 and 313 K) have been evaluated. The process parameters set for this energy analysis are: the liquid flow rate of 60 $ml \cdot min^{-1}$; and the module length of 0.115 m (corresponding to a commercial module, described in Section 2.1. *Experimental: Materials and method*).

The influence of temperature on total energy consumption is found to be negligible. This could be explained due to the fact that higher liquid temperature increases the desorbed CO_2 mass flow rate q_{CO_2}, nearly in proportion to the increase in total work required W_T, due to the increase in temperature. Therefore, the energy consumption of the MVR technology depends mainly on the applied vacuum pressure. On the one hand, W_{vp} increases by 36 % and 41 % for the [emim][Ac] and [emim][MS], respectively, as a consequence of a pressure reduction on the casing side from 0.22 to 0.04 bar. On the other hand, W_{com} and W_{regen} are proportional to the desorbed CO_2 molar flux (G_{vp}).

In this sense, since the increase in W_{vp} with increasing vacuum level is greater than the increase in molar flux across the membrane G_{vp}, the contribution of W_{comp} and W_{regen} decreases markedly for low vacuum pressures.

For [emim][Ac], the contributions of W_{regen} and W_{comp} decrease by 16 % and 3 %, by reducing the vacuum pressure from 0.22 bar to 0.04 bar respectively. In turn, for [emim][MS], the contribution of Wcomp is reduced by 14 %, as a consequence of the same decrease in vacuum pressure.

Table 6 shows the total work required (W_T) for the MVR technology using both ILs ([emim][Ac], [emim][MS]) at four representative operation conditions of vacuum pressure and temperature. The total work of the CO_2 desorption process increased with higher vacuum level applied and higher solvent temperature for both ILs studied in this work (from 7.05E to 06 W to 1.40E-05 W using the chemical IL [emim][Ac] and from 2.55E to 07 W to 5.86E-06 W using physical IL [emim][MS]). Moreover, lower work is required at same condition of vacuum pressure and temperature by using physical IL, mainly due to the absence chemical reaction, wich requires an aditional work (W_{regen}) to desord the CO_2 from the IL. Consequently, regarding the energy consumption, the use of physical IL such as [emim][MS], room temperature and low vacuum level operation should be applied. However, CO_2 desorption performance must be account. For example, for the purpose of obtain a desorption performance equal or higher than 90 % by MVR technology using one membrane contactor, only the chemical IL [emim][Ac] meets the performance requirements by operating the CO_2 desorption process at 0.04 bar of vacuum pressure and 313 K.

Table 6
Total electric work required (W or $J_e \cdot s^{-1}$) at different vacuum levels and temperatures.

***P_V** (bar)*	**0.04**	**0.22**	**0.04**	**0.22**
***T** (K)*	**313**	**313**	**289**	**289**
[emim] [Ac]				
q_{CO_2} ($kg \cdot h^{-1}$, values 10^{-6})	0.08	0.06	0.07	0.05
desorption efficiency(%)	91.44	75.12	78.97	64.88
Work required terms (W, values 10^{-6})				
W_{VP}(W)	6.39	2.30	5.10	1.83
W_{com}(W)	1.25	1.03	1.00	0.82
W_{cool}(W)	0.18	0.06	0.14	0.05
W_{rxn}(W)	6.12	5.03	5.29	4.34
W_T(W)	**14.00**	**8.42**	**11.50**	**7.05**
[emim] [MS]				
q_{CO_2} ($kg \cdot h^{-1}$, values 10^{-7})	0.60	0.06	0.52	0.05
Desorption eff.(%)	74.97	7.67	65.62	6.71
Work required terms (W, values 10^{-7})				
W_{VP}(W)	47.8	2.14	38.6	1.73
W_{com}(W)	9.37	0.96	7.57	0.77
W_{cool}(W)	1.38	0.06	1.11	0.05
W_{regen}(W)	–	–	–	–
W_T(W)	**58.55**	**3.16**	**47.28**	**2.55**

In addition, the total energy consumption E_T, defined as the energy

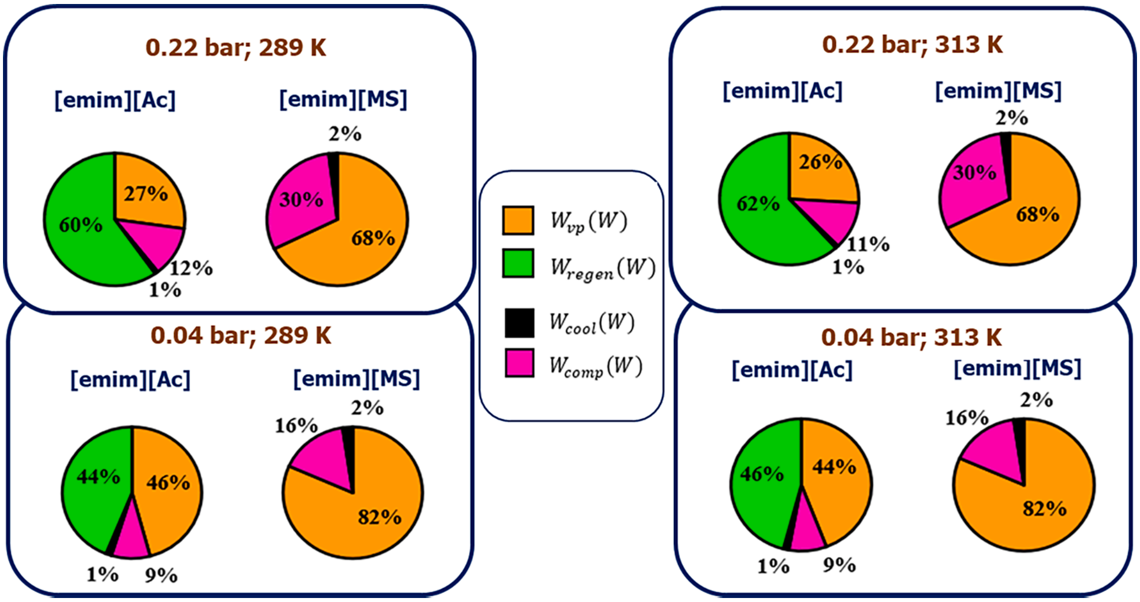

Fig. 9. Contribution (%) to the total CO_2 desorption energy consumption at different operating conditions, of the work needed for the vacuum pump (Wvp), the compressor (Wcom), the vacuum pump cooling (Wcool) and the regeneration heat in terms of equivalent work (Wregen).

required (MJ_e) to desorb 1 kg CO_2 in the IL regeneration process ($MJ_e \cdot kgCO_2^{-1}$), has been evaluated for the two ILs studied in this section. In this regard, Fig. 10 shows the total energy consumption $\boldsymbol{E_T}$, the contribution of the individual energies ($\boldsymbol{E_{VP}}, \boldsymbol{E_{cool}}, \boldsymbol{E_{com}}, \boldsymbol{E_{regen}}$) and the process efficiency for a range of vacuum pressures and temperature of 313 K. From these calculations, the total energy consumption for physical IL [emim][MS] is approximately half of that for chemical IL [emim][Ac] at same vacuum pressure operation, with the compromise of the desorption efficiency.

From these energy calculations, a moderate target of efficiency has been set in order to compare the energy consumption of the desorption process with each of the ILs. In this sense, the efficiency of 75 % has been set as it corresponds to the maximum process efficiency obtained with the IL [emim][MS]. For this moderate target efficiency, the total energy consumption is 0.46 and 0.34 $MJ_e \cdot kgCO_2^{-1}$, for the [emim][Ac] and [emim][MS] respectively.

As a general conclusion, physical ILs could be considered as a promising sorbent for post-combustion capture in terms of energy efficiency. However, further investigation is needed in order to find new physical ILs to improve the performance of the desorption process. On the other hand, chemical ILs with moderate viscosities such as [emim][Ac] provide adequate desorption efficiency to be substitutes for conventional amine-based adsorbents. Moreover, taking into account the continous adsorption–desorption process, the extra work required for the regeneration of the liquid (W_{regen}) could be compensated by the heat generated in the absorption stage, if the same temperature conditions are maintained. In this scenario, a total energy consumption of 0.18 $MJ_e \cdot kgCO_2^{-1}$ is calculated for the [emim][Ac], while the energy consumption of the IL [emim][MS] is kept at 0.34 $MJ_e \cdot kgCO_2^{-1}$ due to the lack of chemical reaction.

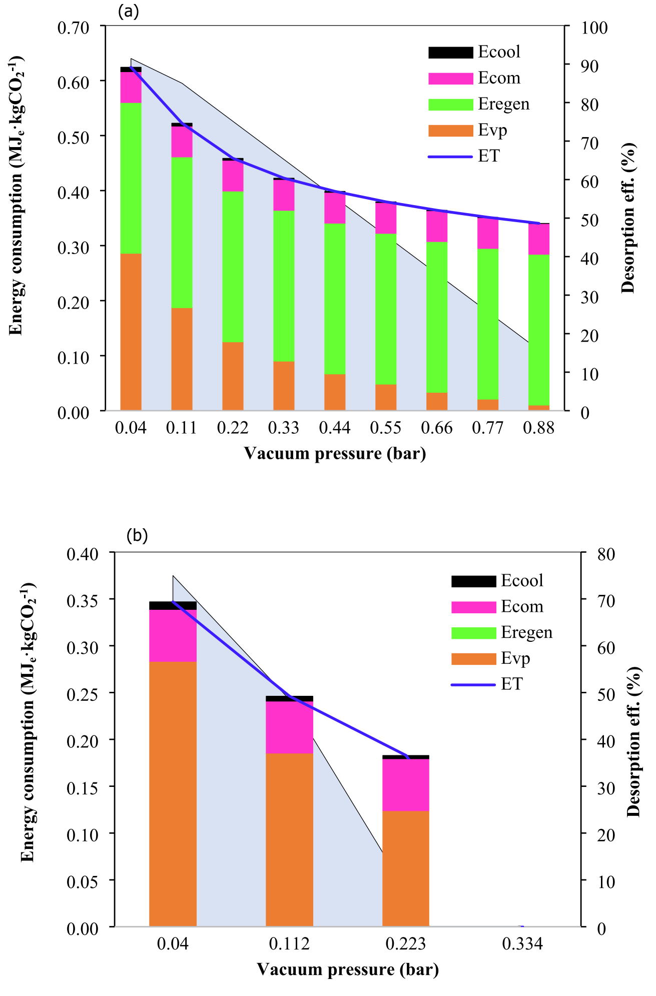

Fig. 10. Total energy consumption ($MJ_e \cdot kgCO_2^{-1}$) at different vacuum pressure levels and 313 K. Chemical [emim][Ac] (a) and physical [emim][MS] (b).

4. Conclusions

The present work contributes to the analysis of the carbon dioxide desorption (based on MVR) in the non-dispersive CO_2 capture and utilization scheme with ILs. Two ILs based on different CO_2 absorption natures, on the one hand, chemical IL [emim][Ac] and on the other hand, the physical [emim][MS], have been studied in terms of process performance and regeneration energy consumption, which is the most energy-intensive stage of the overall CO_2 capture system.

A COSMO-based/Aspen Plus methodology has been performed to carry out the simulations of the CO_2 regeneration stage at different operational conditions. A 2D-mathematical model designed in prior research for the chemical IL [emim][Ac] has been experimentally validated for the physical IL [emim][MS] and exported/integrated from Aspen Custom Modeller (ACM) into the Aspen Plus (AP) simulation software with the COSMO SAC Property Model since there is no HFMC unit in the Aspen Plus model library.

The influence on the CO_2 desorption efficiency and CO_2 desorbed flux of several operation conditions has been carefully analyzed to advance the knowledge of the process. In general, high permeate vacuum level, solvent temperature and fiber length are favorable to the MVR performance while high liquid flow rate increases the CO_2 desorbed flux but also reduce the efficiency of the regeneration process. In particular, the chemical IL [emim][Ac] shows better CO_2 desorption performance and higher CO_2 desorbed flux than physical IL [emim][MS] at all operation conditions studied. The maximum CO_2 desorption efficiencies achieved in this work have been 97 % and 83 % for chemical IL [emim][Ac] and physical IL [emim][MS], respectively. Both performance at 0.04 bar vacuum pressure, 313 K temperature, 60 $ml \cdot min^{-1}$ liquid flowrate and using module-in-series configurations.

Additionally, the energy required by MVR technology to desorb 1 $KgCO_2$ from the CO_2-rich IL has been analyzed at several process conditions of permeate vacuum pressure and solvent temperature. The total energy consumption for physical IL [emim][MS] to reach the maximum CO_2 desorption efficiency (83 %) is about 0.34 $MJ_e \cdot kgCO_2^{-1}$, which is lower to that used chemical IL [emim][Ac] to reach the same regeneration performance (0.52 $MJ_e \cdot kgCO_2^{-1}$). For a set process efficiency of 75 %, a value that can be considered admissible and competitive with the traditional process, the total energy consumption for the ionic liquids [emim][Ac] and [emim][MS] is 0.46 and 0.34 MJ_e-$kgCO_2{}^{-1}$, respectively. However, if process efficiencies higher than 90 % are required, only [emim][Ac] will be suitable. In this sense, it is necessary to find a balance between energy consumption and vacuum desorption performance. Compared with the energy consumption calculated for the conventional regeneration process using amine-based sorbents (1.55 MJ_e-$kgCO_2{}^{-1}$), the results showed in this work for both ILs are promising in terms of energy efficiency, reducing the energy consumption by more than 1 MJ_e-$kgCO_2{}^{-1}$.

This work provides a validated guideline for CO_2 desorption simulations based in MVR technology using both chemical and physical ILs. The process simulation could bring important improvement in the area of solvent selection for CO_2 capture by screening IL performances without extensive experimental work, because of the majority of the ILs are designed and synthesized with complex experimental techniques on laboratory scale, resulting on higher cost in comparison with conventional solvents. From the viewpoint of industrialization, couple membrane technology and IL-based process have been addressed as process intensification technology for CO_2 capture. However, more related simulation studies of the continuous absorption–desorption CO_2 capture system are absolutely essential in the future to push industrial innovation and achieve commercial feasibility of membrane technology and ILs as absorbents. For this purpose, the application of the COSMO-based/

Aspen Plus methodology for simulation of the continuous absorption–desorption CO_2 capture system with all ILs possible is under study in order to evaluate the performances of CO_2 capture process under more realistic process parameters, such as different pressures, temperatures, chemical environments, impurity gases, humidity and mixed-gas feeds. The tool presented here helps in the decision-making to bring the ionic liquids to be implemented in higher technologies readiness levels and consequently be closer to the market.

CRediT authorship contribution statement

Jose Manuel Vadillo: Investigation, Conceptualization, Validation, Formal analysis, Data curation, Writing – original draft. **Lucia Gomez-Coma:** Supervision, Methodology, Writing – review & editing. **Aurora Garea:** Conceptualization, Methodology, Writing – review & editing, Funding acquisition. **Angel Irabien:** Supervision, Conceptualization, Project administration, Writing – review & editing, Funding acquisition.

Declaration of Competing Interest

The authors declare that they have no known competing financial interests or personal relationships that could have appeared to influence the work reported in this paper.

Acknowledgements

This work has been funded by the Spanish Ministry of Economy, Industry and Competitiveness (MINECO), project CTQ2016-76231-C2-(AEI/FEDER, UE), project PID2019-108136RB-C31-(MCIN/AEI) and project PID2020-112845RB-I00-(MCIN/AEI). J.M.V. thanks the Concepción Arenal postgraduate research grant from the University of Cantabria.

References

[1] Life Cycle Engineering Turin, CORDIS EU Research Results, European Commission, 2020.

[2] G. Díaz-sainz, M. Alvarez-guerra, J. Solla-gullón, L. García-cruz, V. Montiel, A. Irabien, CO_2 electroreduction to formate: Continuous single-pass operation in a filter-press reactor at high current densities using Bi gas diffusion electrodes, J. CO_2 Utilizat. 34 (2019) 12–19, https://doi.org/10.1016/j.jcou.2019.05.035.

[3] T. Li, T.C. Keener, A review: Desorption of CO_2 from rich solutions in chemical absorption processes, Int. J. Greenhouse Gas Control 51 (2016) 290–304, https://doi.org/10.1016/j.ijggc.2016.05.030.

[4] H. Nieminen, L. Järvinen, V. Ruuskanen, A. Laari, T. Koiranen, J. Ahola, Insights into a membrane contactor based demonstration unit for CO_2 capture, Sep. Purif. Technol. 231 (2020), 115951, https://doi.org/10.1016/j.seppur.2019.115951.

[5] N. Intan Listiyana, Y. Rahmawati, S. Nurkhamidah, H. Rofiq Syahnur, Y. Zaelana, CO_2 desorption from activated DEA using membrane contactor with vacuum regeneration technology, MATEC Web Conferences 156 (2018), https://doi.org/10.1051/matecconf/201815608012.

[6] Q. He, J. Xi, W. Wang, L. Meng, S. Yan, CO_2 absorption using biogas slurry: Recovery of absorption performance through CO_2 vacuum regeneration, Int. J. Greenhouse Gas Control 58 (2017) 103–113, https://doi.org/10.1016/j.ijggc.2017.01.010.

[7] J.M. Vadillo, L. Gomez-Coma, A. Garea, A. Irabien, Hollow Fiber Membrane Contactors in CO_2 Desorption: A Review, Energy Fuels 35 (2021) 111–136, https://doi.org/10.1021/acs.energyfuels.0c03427.

[8] D.A. Zaidiza, B. Belaissaoui, S. Rode, E. Favre, Intensification potential of hollow fiber membrane contactors for CO_2 chemical absorption and stripping using monoethanolamine solutions, Sep. Purif. Technol. 188 (2017) 38–51, https://doi.org/10.1016/j.seppur.2017.06.074.

[9] H.J. Lee, M.K. Kim, J.H. Park, Decompression stripping of carbon dioxide from rich monoethanolamine through porous hydrophobic modified ceramic hollow fiber membrane contactor, Sep. Purif. Technol. 236 (2020), 116304, https://doi.org/10.1016/j.seppur.2019.116304.

[10] P. Kosaraju, A.S. Kovvali, A. Korikov, K.K. Sirkar, Hollow fiber membrane contactor based CO_2 absorption-stripping using novel solvents and membranes, Ind. Eng. Chem. Res. 44 (2005) 1250–1258, https://doi.org/10.1021/ie0495630.

[11] M. Fang, Z. Wang, S. Yan, Q. Cen, Z. Luo, CO_2 desorption from rich alkanolamine solution by using membrane vacuum regeneration technology, Int. J. Greenhouse Gas Control 9 (2012) 507–521, https://doi.org/10.1016/j.ijggc.2012.05.013.

[12] S. Yan, M. Fang, Z. Wang, Z. Luo, Regeneration performance of CO_2-rich solvents by using membrane vacuum regeneration technology: Relationships between absorbent structure and regeneration efficiency, Appl. Energy 98 (2012) 357–367, https://doi.org/10.1016/j.apenergy.2012.03.055.

[13] Z. Wang, M. Fang, Y. Pan, S. Yan, Z. Luo, Amine-based absorbents selection for CO_2 membrane vacuum regeneration technology by combined absorption-desorption analysis, Chem. Eng. Sci. 93 (2013) 238–249, https://doi.org/10.1016/j.ces.2013.01.057.

[14] S. Nii, Y. Iwata, K. Takahashi, H. Takeuchi, Regeneration of CO_2-loaded carbonate solution by reducing pressure, J. Chem. Eng. Jpn. 28 (1995) 148–153, https://doi.org/10.1252/jcej.28.148.

[15] A. Rosli, N.F. Shoparwe, A.L. Ahmad, S.C. Low, J.K. Lim, Dynamic modelling and experimental validation of CO_2 removal using hydrophobic membrane contactor with different types of absorbent, Sep. Purif. Technol. 219 (2019) 230–240, https://doi.org/10.1016/j.seppur.2019.03.030.

[16] X. Yan, S. Anguille, M. Bendahan, P. Moulin, Ionic liquids combined with membrane separation processes: A review, Sep. Purif. Technol. 222 (2019) 230–253, https://doi.org/10.1016/j.seppur.2019.03.103.

[17] P.J. Carvalho, K.A. Kurnia, J.A.P. Coutinho, Dispelling some myths about the CO_2 solubility in ionic liquids, PCCP 18 (2016) 14757–14771, https://doi.org/10.1039/C6CP01896C.

[18] Q. Sohaib, J.M. Vadillo, L. Gómez-Coma, J. Albo, S. Druon-Bocquet, A. Irabien, J. Sanchez-Marcano, Post-combustion CO_2 capture by coupling [emim] cation based ionic liquids with a membrane contactor; Pseudo-steady-state approach, Int. J. Greenhouse Gas Control 99 (2020), 103076, https://doi.org/10.1016/j.ijggc.2020.103076.

[19] T. Mulukutla, G. Obuskovic, K.K. Sirkar, Novel scrubbing system for post-combustion CO_2 capture and recovery: Experimental studies, J. Membr. Sci. 471 (2014) 16–26, https://doi.org/10.1016/j.memsci.2014.07.037.

[20] S. Bazhenov, A. Malakhov, D. Bakhtin, V. Khotimskiy, G. Bondarenko, V. Volkov, M. Ramdin, T.J.H. Vlugt, A. Volkov, CO_2 stripping from ionic liquid at elevated pressures in gas-liquid membrane contactor, Int. J. Greenhouse Gas Control 71 (2018) 293–302, https://doi.org/10.1016/j.ijggc.2018.03.001.

[21] J.G. Lu, Z.Y. Lu, Y. Chen, J.T. Wang, L. Gao, X. Gao, Y.Q. Tang, D.G. Liu, CO_2 absorption into aqueous blends of ionic liquid and amine in a membrane contactor, Sep. Purif. Technol. 150 (2015) 278–285, https://doi.org/10.1016/j.seppur.2015.07.010.

[22] T.J. Simons, P. Hield, S.J. Pas, A novel experimental apparatus for the study of low temperature regeneration CO_2 capture solvents using hollow fibre membrane contactors, Int. J. Greenhouse Gas Control 78 (2018) 228–235, https://doi.org/10.1016/j.ijggc.2018.08.009.

[23] J.M. Vadillo, L. Gómez-coma, A. Garea, A. Irabien, CO_2 Desorption Performance from Imidazolium Ionic Liquids by Membrane Vacuum Regeneration Technology, Membranes (Basel) 10 (2020) 234. 10.3390/membranes10090234.

[24] D. Hospital-Benito, J. Lemus, C. Moya, R. Santiago, J. Palomar, Process analysis overview of ionic liquids on CO_2 chemical capture, Chem. Eng. J. 390 (2020), 124509, https://doi.org/10.1016/j.cej.2020.124509.

[25] S. Zhao, P.H.M. Feron, L. Deng, E. Favre, E. Chabanon, S. Yan, J. Hou, V. Chen, H. Qi, Status and progress of membrane contactors in post-combustion carbon capture: A state-of-the-art review of new developments, J. Membr. Sci. 511 (2016) 180–206, https://doi.org/10.1016/j.memsci.2016.03.051.

[26] S. Qazi, L. Gómez-coma, J. Albo, S. Druon-bocquet, A. Irabien, Mathematical Modelling of CO2 Absorption with Ionic Liquids in a Membrane Contactor, Study of Absorption Kinetics and Influence of Temperature, J. Chem. Technol. Biotechnol. (2019), https://doi.org/10.1002/jctb.6265.

[27] M. Ramdin, T.W. De Loos, T.J.H. Vlugt, State-of-the-art of CO_2 capture with ionic liquids, Ind. Eng. Chem. Res. 51 (2012) 8149–8177, https://doi.org/10.1021/ie3003705.

[28] R. Sander, Modeling atmospheric chemistry: interactions between gas-phase species and liquid cloud/aerosol particles, Surv. Geophys. 20 (1999) 1–31. 10.1023/A:1006501706704.

[29] S. Qazi, J. Manuel Vadillo, L. Gómez-Coma, J. Albo, S. Druon-Bocquet, A. Irabien, J. Sanchez-Marcano, CO2 Capture with Room Temperature Ionic Liquids; Coupled Absorption/Desorption and Single Module Absorption in Membrane Contactor, Chem. Eng. Sci. 223 (2020) 115719, https://doi.org/10.1016/j.ces.2020.115719.

[30] V.R. Ferro, E. Ruiz, M. Tobajas, J.F. Palomar, Integration of COSMO-Based Methodologies Into Commercial Process Simulators: Separation and Purification of Reuterin, AIChE J. (2012), https://doi.org/10.1021/ie070465z.

[31] J. Palomar, M. Larriba, J. Lemus, D. Moreno, R. Santiago, C. Moya, J. De Riva, G. Pedrosa, Demonstrating the key role of kinetics over thermodynamics in the selection of ionic liquids for CO_2 physical absorption, Sep. Purif. Technol. 213 (2019) 578–586, https://doi.org/10.1016/j.seppur.2018.12.059.

[32] J.M. Vadillo, D. Hospital-benito, C. Moya, L. Gomez-, J. Palomar, A. Garea, A. Irabien, Modelling and simulation of hollow fiber membrane vacuum regeneration for CO_2 desorption processes using ionic liquids, Sep. Purif. Technol. (2021), 119465, https://doi.org/10.1016/j.seppur.2021.119465.

[33] F. Zareiekordshouli, A. Lashanizadehgan, P. Darvishi, Experimental and theoretical study of CO_2 solubility under high pressure conditions in the ionic liquid 1-ethyl-3-methylimidazolium acetate, J. Supercrit. Fluids 133 (2018) 195–210, https://doi.org/10.1016/j.supflu.2017.10.008.

[34] M.B. Shiflett, A. Yokozeki, Phase behavior of carbon dioxide in ionic liquids: [emim][acetate], [emim][trifluoroacetate], and [emim][acetate] + [emim][trifluoroacetate] mixtures, J. Chem. Eng. Data 54 (2009) 108–114, https://doi.org/10.1021/je800701j.

[35] V.R. Ferro, C. Moya, D. Moreno, R. Santiago, J. De Riva, G. Pedrosa, M. Larriba, I. Diaz, J. Palomar, Enterprise Ionic Liquids Database (ILUAM) for Use in Aspen ONE Programs Suite with COSMO-Based Property Methods, Ind. Eng. Chem. Res. 57 (2018) 980–989, https://doi.org/10.1021/acs.iecr.7b04031.

[36] P. García-Gutiérrez, J. Jacquemin, C. McCrellis, I. Dimitriou, S.F.R. Taylor, C. Hardacre, R.W.K. Allen, Techno-Economic Feasibility of Selective CO_2 Capture Processes from Biogas Streams Using Ionic Liquids as Physical Absorbents, Energy Fuels 30 (2016) 5052–5064, https://doi.org/10.1021/acs.energyfuels.6b00364.

[37] G. Díaz-Sainz, M. Alvarez-Guerra, J. Solla-Gullón, L. García-Cruz, V. Montiel, A. Irabien, Catalyst coated membrane electrodes for the gas phase CO_2 electroreduction to formate, Catal. Today 346 (2018) 58–64, https://doi.org/10.1016/j.cattod.2018.11.073.

[38] Z. Wang, M. Fang, Q. Ma, Z. Zhao, T. Wang, Z. Luo, Membrane stripping technology for CO_2 desorption from CO_2-rich absorbents with low energy consumption, Energy Proc. 63 (2014) 765–772, https://doi.org/10.1016/j.egypro.2014.11.085.

[39] H. Kim, S.J. Hwang, K.S. Lee, Novel Shortcut Estimation Method for Regeneration Energy of Amine Solvents in an Absorption-Based Carbon Capture Process, Environ. Sci. Technol. 49 (2015) 1478–1485, https://doi.org/10.1021/es504684x.

[40] N. Matsumiya, M. Teramoto, S. Kitada, H. Matsuyama, Evaluation of energy consumption for separation of CO_2 in flue gas by hollow fiber facilitated transport membrane module with permeation of amine solution, Sep. Purif. Technol. 46 (2005) 26–32, https://doi.org/10.1016/j.seppur.2005.04.006.

[41] S. Yan, M. Fang, Z. Luo, K. Cen, Regeneration of CO_2 from CO_2-rich alkanolamines solution by using reduced thickness and vacuum technology: Regeneration feasibility and characteristic of thin-layer solvent, Chem. Eng. Process. 48 (2009) 515–523, https://doi.org/10.1016/j.cep.2008.06.009.

[42] D. Albarracin-Zaidiza, B. Belaissaoui, D. Roizard, E. Favre, S. Rode, Stripping of CO_2 in Post-combustion Capture with Chemical Solvents: Intensification Potential of Hollow Fiber Membrane Contactors, Energy Proc. 114 (2017) 1334–1341, https://doi.org/10.1016/j.egypro.2017.03.1254.

[43] M.B. Shiflett, B.A. Elliott, S.R. Lustig, S. Sabesan, M.S. Kelkar, A. Yokozeki, Phase behavior of CO_2 in room-temperature ionic liquid 1-ethyl-3-ethylimidazolium acetate, ChemPhysChem 13 (2012) 1806–1817, https://doi.org/10.1002/cphc.201200023.

[44] J.H. Yim, S.J. Ha, J.S. Lim, Measurement and Correlation of CO_2 Solubility in 1-Ethyl-3-methylimidazolium ([EMIM]) Cation-Based Ionic Liquids: [EMIM][Ac], [EMIM][Cl], and [EMIM][MeSO4], J. Chem. Eng. Data 63 (2018) 508–518, https://doi.org/10.1021/acs.jced.7b00532.

[45] J. Palomar, V.R. Ferro, J.S. Torrecilla, F. Rodríguez, Density and molar volume predictions using COSMO-RS for ionic liquids. An approach to solvent design, Ind. Eng. Chem. Res. 46 (2007) 6041–6048, https://doi.org/10.1021/ie070445x.

[46] L. Zhou, X. Shang, J. Fan, J. Wang, Solubility and selectivity of CO_2 in ether-functionalized imidazolium ionic liquids, J. Chem. Thermodyn. 103 (2016) 292–298, https://doi.org/10.1016/j.jct.2016.08.028.

[47] J.G. Lu, C.T. Lu, Y. Chen, L. Gao, X. Zhao, H. Zhang, Z.W. Xu, CO_2 capture by membrane absorption coupling process: Application of ionic liquids, Appl. Energy 115 (2014) 573–581, https://doi.org/10.1016/j.apenergy.2013.10.045.